22.1: *Invited Paper:* Technological Challenges for Large-Size AMOLED Display

Hye Dong Kim, Jae Kyeong Jeong, Hyun-Joong Chung and Yeon-Gon Mo
Corporate R&D center, Samsung SDI Co. LTD,
428-5, Gongse-Dong, Kiheung-Ku, Yongin-City, Kyungki-Do, 449-577, Korea

Abstract
In this work, we review the current technological challenges for large-size AMOLED displays with an emphasis on the backplane technology. Then, it will be discussed how the new technology of oxide TFTs combines the advantages of LTPS and a-Si TFTs to make an optimal solution for large-size backplanes. In particular, we reveal the technological challenges in oxide TFTs by comparing the device characteristics of conventional excimer laser annealing (ELA) LTPS and amorphous indium-gallium-zinc-oxide (a-IGZO) TFTs. Finally, we demonstrate a 12.1" WXGA AMOLED prototype display fabricated by an a-IGZO TFT backplane.

1. Introduction
Among existing display technologies, active-matrix organic light-emitting diodes (AMOLEDs) provide the best solution to achieve 'ultimate display' due to their fast motion picture response time, vivid color, high contrast, and super-slim, lightweight nature [1,2]. In 2007, Samsung SDI has launched the first mass production of small-sized AMOLEDs for cell-phone and MP4 displays. The market is now burgeoning for mid-to-large-size applications, for example, note PC, monitor, and televisions. Samsung SDI's recent exhibition of 14-inch and 31-inch full HD television prototype [3] and Sony's commercialization of qFHD 11-inch TV (XEL-1) clearly show that the era of AMOLED TV is indeed nearby. Whereas the market is projected to reach 54 million units by 2011 [4], a number of hurdles in technology should be overcome for the mass production of mid-to-large sized AMOLED panels.

In order to mass-produce large-size AMOLED with affordable price, the size of mother glass should be increased at least to Gen. 5.5. Naturally, the scaling-up of the production line causes several technological challenges. The challenges can be categorized into three parts; TFT performance and fabrication, OLED patterning, and encapsulation. In this introduction, we briefly review the current status and critical issue of each part. Firstly, ELA-based LTPS TFT, which are used as a backplane for AMOLED displays due to their high mobility (>80 cm^2/Vs) and stability, suffer from the non-uniformity of their mobility and threshold voltage, due to the existence of grain boundaries. Moreover, the enlargement of substrate (>Gen. 5.5) is limited due to the small laser beam size and rather long process tact time. The more detail concerning TFT technology will be described in the next section. Secondly, regarding patterning OLED device, fine metal shadow mask (FMM) has been the only commercialized patterning method used in color primaries of OLED. However, FMM has an intrinsic limit of mechanical bending when the size is increased. To circumvent the problem, sequential pattern formation can be implemented, but the method has weakness in uniformity and tact time. Inkjet printings of soluble OLED material [5] and color filter on white OLED [6] are alternative candidates, but their performance is limited by the immaturity of OLED materials and the complexity of sustaining stable white light, respectively. Laser-based patterning methods, such as radiation-induced sublimation transfer (RIST) [7], laser-induced pattern-wise sublimation (LIPS) [8], and laser-induced thermal transfer (LITI) [2] are strong candidates to replace FMM. Samsung SDI and 3M have co-developed LITI technology to implement both towards high-definition patterning (>300ppi) and large-size glasses. Finally, encapsulation is another important issue for large-size displays. Encapsulation is necessary to prevent degradation of OLED from the attack of oxygen and moisture from atmosphere. Regarding that the HDTV require at least 40,000 to 50,000 hour lifetime, the development of simple but reliable encapsulation method is unquestionable.

In this paper, we will discuss how the new technology of oxide TFTs allows simple solution for the challenges in backplane technologies for large-size AMOLED displays by reviewing the current issues in scaling-up the AMOLED backplanes. Then, the current challenges in oxide TFT fabrication are shown.

2. Current Status and Issues on Crystallization Technology
The four major concerns in OLED backplanes are the reduction of photo-mask numbers, the improvement of brightness non-uniformity, IR drop prevention, and device reliability. Amorphous silicon (a-Si) TFTs, currently employed in liquid crystal display (LCD) industry nowadays, have the merit of easy fabrication and size scalability, thus simple 4-mask fabrication on Gen. 8 glass is possible for AMLCDs. However, because of intrinsically poor mobility (<1 cm^2/V.s) and device instability, a-Si TFTs have scarcely been used for AMOLED backplanes. Instead, low-temperature polycrystalline Si (LTPS) provides high mobility (up to 200 cm^2/Vs) and stable TFTs. The key process in fabricating LTPS TFTs is the crystallization methods that convert a-Si into polycrystalline Si. These methods can be classified to non-laser (thermal) crystallization and laser annealing. Among non-laser crystallization, the simplest method is solid phase crystallization (SPC). But SPC requires 600ºC annealing for tens of hours, whick makes it not suitable for large-area glass substrates. Other non-laser methods employ metal seed for crystallization, which may cause large leakage current in channel area. Among laser methods, excimer laser annealing (ELA; see Figure 1) has been the most widely used due to its excellent crystallinity, fast crystallization speed, and high mobility. In addition, ELA is already employed in mass-production, thus well-developed apparatuses are commercially available. However, ELA suffers from the narrow process window, high initial investment and maintenance cost. Especially, the limitation in laser beam length and the laser beam instability are the major obstacles to use ELA on large-sized glass. In addition, the rough surface of ELA LTPS surface can lower the breakdown voltage of gate insulator, consequently causing the failure of TFT device during operation. An alternative solution employing laser

can be sequential laser solidification (SLS), but there is still an issue regarding brightness non-uniformity on OLED panel [1]. In fact, all LTPS TFTs suffer from the non-uniformity issue because of the existence of grain boundaries. Recently, micro-crystalline Si draws attention to replace LTPS [9], but it still requires the high cost laser apparatus.

As an alternative solution for the large-size AMOLED display backplanes, amorphous oxide TFTs provide unique properties that combine the advantages of a-Si and LTPS TFTs. For example, amorphous oxide TFTs are free from the non-uniformity of mobility and threshold voltage, yet exhibits large carrier mobility (~10cm^2/Vs) and excellent subthreshold gate swing (down to 0.20 V/dec). Moreover, the channel layer can be fabricated by simple sputtering process, as shown in Figure 2. Therefore, large-size fabrication can be easily implemented without using expensive laser apparatus. The process route is essentially the same as a-Si TFTs so that the existing production line can be used without significant change. In addition, oxide TFTs can be deposited at room temperature, which, in principle, makes it possible the mass production of AMOLEDs on flexible plastic substrates or cheap soda-lime glass.

In this paper, the structure and the process of amorphous indium-gallium-zinc-oxide (a-IGZO) TFT is introduced. Then, representative device performances are compared to ELA TFTs. Finally, the device stability issue in IGZO TFT is discussed.

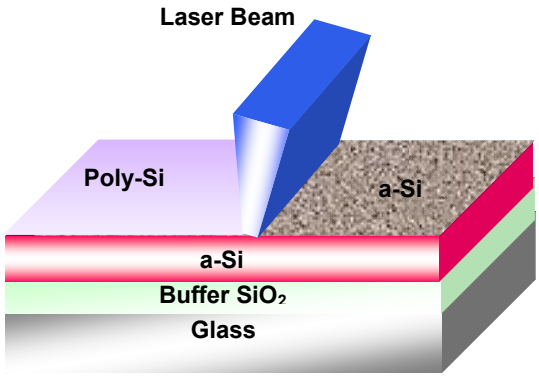

Figure 1. The schematic diagram of ELA crystallization in LTPS TFT

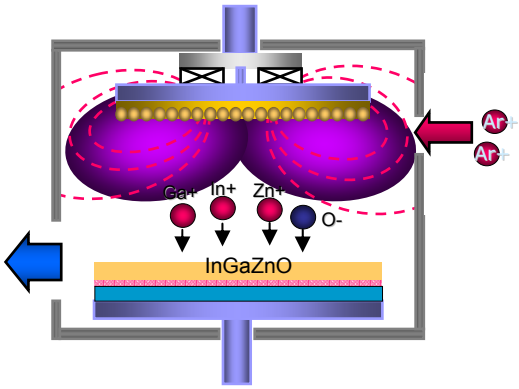

Figure 2. The schematic diagram of the sputtering system of IGZO channel layer in oxide TFT.

3. Oxide TFT Technology

3.1 TFT Structure

Figure 3 shows the schematic cross section of the IGZO TFTs, which have an inverted staggered bottom gate architecture with an etch stopper layer (ESL). For an a-IGZO TFT without an ESL, severe degradation of the subthreshold gate swing (SS) and the uniformity of threshold voltage (V_{th}) were observed. This is why we chose ESL-type structure rather than back-channel etch structure (BCE-type), which is generally adopted for liquid crystal display.

Lithographically patterned Mo (200nm) on a SiO_2/glass substrate with a surface area of 370×400 mm^2 was used as the gate electrode. Either SiO_x film or SiO_x/SiN_x bi-layer film as a gate dielectric layer was deposited by plasma enhanced chemical vapor deposition (PECVD) at 390°C. The a-IGZO film was grown by sputtering on the SiO_2/glass substrate using a polycrystalline $In_2Ga_2ZnO_7$ target at room temperature. After defining the a-IGZO channel using photolithography and wet etching, a SiO_x etch stopper was deposited by PECVD and then, patterned by dry etching. As a source and drain electrode, either Mo or Ti/Al/Ti material was formed by sputtering and defined by photolithography and then patterned by dry etching. The device characteristics of the a-IGZO TFTs were measured at room temperature with an Agilent 4156C precision semiconductor parameter analyzer.

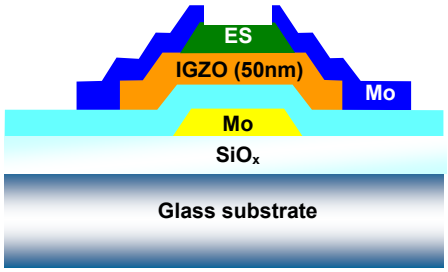

Figure 3. The schematic cross-section of a-IGZO TFT.

3.2 Device Characteristics

Figure 4 shows the representative transfer characteristics of a-IGZO TFTs with W/L = 25/10μm. The threshold voltage ($V_{th,sat}$) was defined by the gate voltage, which induces a drain current of L/W×10 nA at a V_{DS} of 5.1 V. The apparent field-effect mobility induced by the transconductance at a low drain voltage (V_{DS} ≤ 1 V) is determined by

$$\mu_{FE} = \frac{Lg_m}{WC_iV_{DS}}$$

where C_i and g_m are the gate capacitance per unit area and the transconductance, respectively.

The *a*-IGZO TFT with an ESL exhibited a field-effect mobility of 8.0 cm^2/V s, an *S* value of 0.53 V/decade, a $V_{th,sat}$ of 2.4 V, and an $I_{on/off}$ of > 2.0×10^7. It is evident that the overall device performances of amorphous oxide TFT are better than those of microcrystalline Si and amorphous Si TFT. These better characteristics of a-IGZO TFT were reflected in the excellent

output characteristics of the device, which exhibited a clear pinch-off and drain current saturation (not shown).

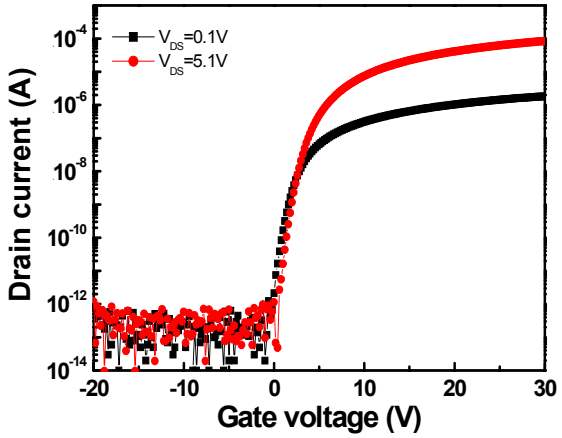

Figure 4. The representative transfer curve of the a-IGZO TFT with W/L=25/10μm with ESL.

3.3 Device Stabilities

In general, the surface roughness of poly-Si film can significantly affect the integrity of the gate insulator in the resulting TFT. Figure 5 shows the gate leakage current density as a function of gate electrical field for ELA and oxide TFT. The electrical breakdown field of gate insulator for ELA was less than 6.5MV/cm, which can be correlated to the protrusion formation of Si grain boundary during laser crystallization. However, in case of oxide TFT, the electrical breakdown field of gate insulator was >10MV/cm, because the interface between IGZO channel layer and gate dielectric layer was very smooth.

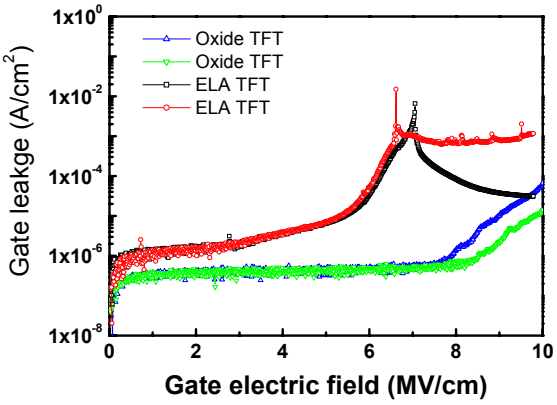

Figure 5. The gate leakage current density as a function of the applied gate electric field for ELA and oxide TFT. The thickness of bi-layer gate dielectric was identical to 120nm.

In AMOLED device, the driving transistors act as the analog driver of the constant current source. Therefore, the stability of TFT is one of the key factors, which should be robust under the various stress conditions. The effect of the various gate voltage stresses on the transfer characteristics for ELA and oxide TFT (W/L=7/7μm) was shown in Fig. 6(a) and (b), respectively. The initial device parameters were summarized in Table 1. During gate-bias stressing, the source and drain were grounded, and a positive voltage (10, 15, 20V) was applied to the gate for 600s. In the case of ELA TFT, there is no V_{th} shift when the gate voltage was applied less than 15V. However, the V_{th} shifted positively approximately by 0.5V at the gate voltage of 20V. On the other hand, the V_{th} shift of oxide TFT was more severe: the V_{th} of oxide TFT changed by 1.2V at the gate voltage stress of 15V. Interestingly, there is no degradation of field-effect mobility and threshold gate swing after the gate voltage stress. Therefore, the V_{th} instability seems to be related to the temporal charge trapping at the interface of oxide channel and gate insulator, even though the physical and electrical origin of the device instability is not clear. It should be noted that the stability of oxide TFT is much better than that of a-Si TFT (not shown). The studies on the mechanism of V_{th} degradation are being under investigation and the process and circuit design development for the improvement of V_{th} instability is currently undergoing.

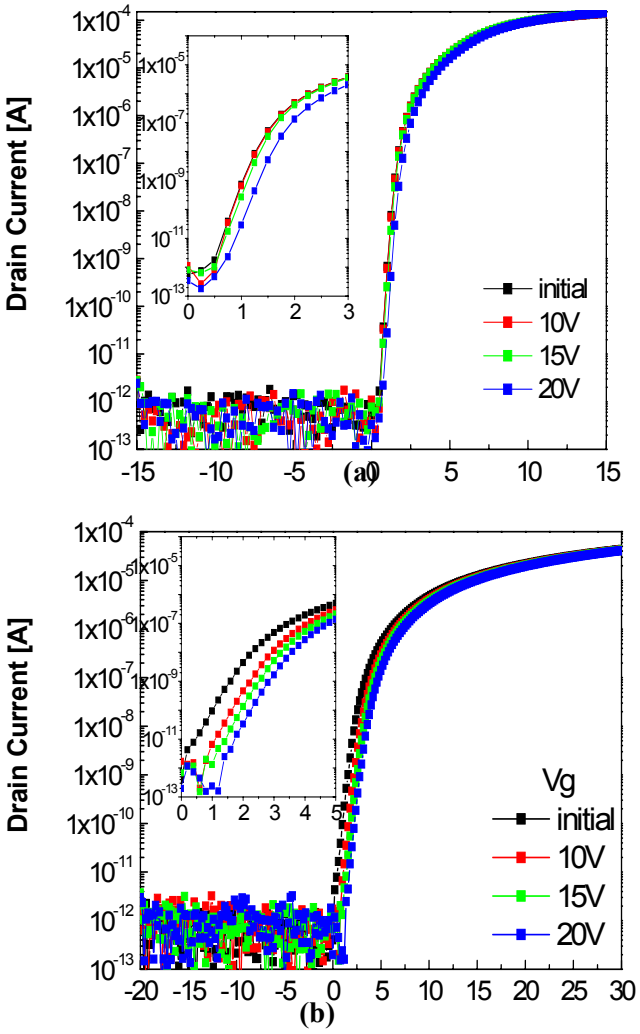

Figure 6(a) and (b) show the effect of the various gate voltage stresses on the transfer characteristics for ELA and oxide TFT, respectively.

	Vth [V]	SS [V/dec]	Mobility [cm^2/V.s]	Ion [μA/μm]
ELA TFT	1.3	0.24	102	28.4
Oxide TFT	2.0	0.54	9.3	0.97

Table 1. Initial TFT parameters extracted from Figure 6.

4. 12.1-inch AMOLED Prototype

In this work, we have successfully developed a full-color 12.1-inch WXGA AMOLED display, which was driven by a-IGZO TFTs backplane. The display has the pixel number of 1280×RGB×768 with the resolution of 123ppi. Its sub-pixel pitch is the 69× 207μm^2 and the pixel element of 2Tr and 1cap. The channel length for driving transistor was designed to 10μm, but the kink effect, which appears in poly-Si TFT with the same channel length, was not observed in output characteristics. The scan driver was integrated on the panel and its functionality was successfully demonstrated. Figure 7 shows an image of the 12.1" WXGA AMOLED display.

Recently, LG Electronic reported the 3.5-inch QCIF$^+$ AMOLED prototype, which was driven by a-IGZO TFTs backplane [11]. We have also reported 4.1-inch transparent QCIF AMOLED display using a-IGZO TFTs in IMID 2007 [12]. So far, the research and development for a-IGZO TFTs has been focused on the demonstration of rather small-size AMOLED (<5inch). It should be emphasized that our prototype is the largest and highest resolution AMOLED display using a-IGZO TFTs backplane.

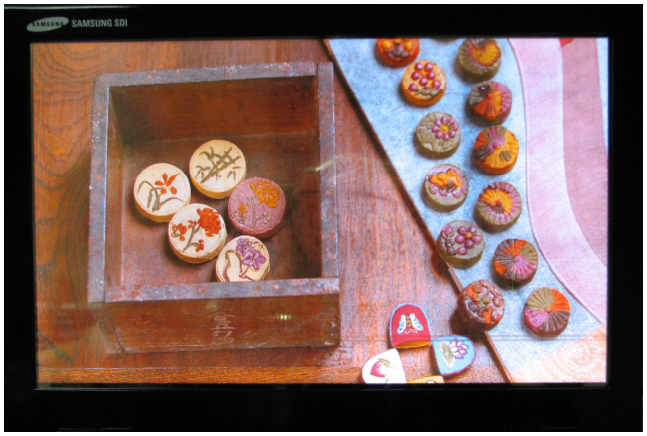

Figure 7. The display image of 12.1" WXGA AMOLED display.

5. Summary

In order to expand the AMOLED market, the size of mother glass substrate should be increased at least up to Gen. 5.5 to produce cost-effective note-PC, monitor, and HDTV. Whereas conventional ELA-based backplane technology is facing strong challenge on the glass size scalability, a-IGZO TFTs can be easily expanded into large size substrate (>Gen. 7) by using conventional sputtering technique for channel fabrication. Our demonstration of 12.1" WXGA shows that the a-IGZO TFTs can possibly replace conventional LTPS-based backplane technologies.

6. Acknowledgements

The authors appreciate K. N. Kim and K. N. Kang who designed layout and simulated circuit for 12.1" panel and B. S. Gu for module test. The author would like to thank all the project members in Samsung SDI.

7. References

[1] H. K. Chung and K. Y. Lee, SID '05 Digest, pp. 956-959 (2005).

[2] S. T. Lee, M. C. Suh, T. M. Kang, Y. G. Kwon, J. H. Lee, H. D. Kim, and H. K. Chung, SID '07 Digest, pp. 1588-1591 (2007).

[3] Exhibited in CES 2008.

[4] Source: Display Bank ('07,2Q), http://www.displaybank.com

[5] T. Gohda, Y. Kobayashi, K. Okano, S. Inoue, K. Okamoto, S. Hashimoto, E. Yamamoto, H. Morita, S. Mitsui, and M. Koden, SID '06 Digest, pp. 1767-1770 (2006).

[6] K. Chung, N. Kim, J. Choi, C. Chu, and J.-M. Huh, SID '06 Digest, pp. 1958-1963 (2006).

[7] M. Boroson, L. Tutt, K. Nguyen, D. Preuss, M. Culver, and G. Phelan, SID '05 Digest, pp. 972-975 (2005).

[8] T. Hirano, K. Matsuo, K. Kohinata, K. Hanawa, T. Matsumi, E. Matsuda, R. Matsuura, T. Ishibashi, A. Yoshida, and T. Sasaoka, SID '07 Digest, pp. 1592-1595 (2007).

[9] T. Arai, N. Morosawa, Y. Hiromasu, K. Hidaka, T. Nakayama, A. Makita, M. Toyota, N. Hayashi, Y. Yoshimura, A. Sato, K. Namekawa, Y. Inagaki, N. Umezu, and K. Tatsuki, SID '07 Digest, pp. 1370-1373 (2007).

[10] M. Kim, J. H. Jeong, H. J. Lee, T. K. Ahn, H. S. Shin, J. -S. Park, J. K. Jeong, Y.-G. Mo, and H. D. Kim, Appl. Phys. Lett. 90, 212114 (2007).

[11] H. N. Lee, J. W. Kyung, S. K. Kang, D. Y. Kim, M. C. Sung, S. J. Kim, C. N. Kim, H. G. Kim, and S. T. Kim, Proc. IDW, Otsu, Japan, pp. 663-666 (2007).

[12] J. K. Jeong, M. Kim, J. H. Jeong, H. J. Lee, T. K. Ahn, H. S. Shin, K. Y. Kang, H. Seo, J. S. Park, H. Yang, H. J. Chung, Y. G. Mo, and H. D. Kim, Proc. IMID, Daegu, Korea, pp. 145-148 (2007).